ELSEVIER

Journal of Alloys and Compounds 271–273 (1998) 850–853

Journal of ALLOYS AND COMPOUNDS

Spectroscopy and dynamics of 5f states of Es^{3+} in LaF_3

James V. Beitz*, Clayton W. Williams, G.K. Liu

Chemistry Division, Argonne National Laboratory, Argonne, IL 60439, USA

Abstract

Using time- and wavelength-resolved laser-induced fluorescence methods, the 5f state spectroscopy and photodynamics of $^{253}Es^{3+}$ in LaF_3 have been investigated. Based on an effective operator Hamiltonian model and approximating the metal ion site symmetry as C_{2v}, a set of crystal field parameters has been obtained that fit the 56 assigned levels associated with the seven states of Es^{3+} that were observed. The $^5F_5$ emitting state of Es^{3+} exhibited a decay rate that approached the expected purely radiative decay of the state. This suggests that the shorter lifetime previously found for this state of Es^{3+} in $LaCl_3$ arose from radiation damage induced by α decay of ^{253}Es.

Keywords: Einsteinium; Spectroscopy; Photophysics; Crystal field theory

---

1. Introduction

Past investigations [1] of the 5f state energy level structure of Es^{3+} focused on $LaCl_3$ as the host because of the prior extensive experimental spectroscopy and modeling efforts for trivalent lanthanide ions (Ln^{3+}) ions in $LaCl_3$ [2]. This past work both enabled rapid identification of transitions due to rare earth impurities in $LaCl_3$ and provided a starting point for theoretical modeling. Similarly detailed work for Ln^{3+} ions in LaF_3 was published recently [3]. Our current investigation marks the beginning of 5f state spectroscopy and photophysics studies on trivalent actinides in LaF_3.

The synthesis, nuclear properties, and purification of Es have been reviewed by Hulet [4]. Radiation damage rapidly accumulates in hosts that contain ^{253}Es because it is a short-lived ($t_{1/2}=20.47$ days) α emitter. In consequence, color center formation and other radiation damage-related factors may account for an observed luminescence lifetime of $^{253}Es^{3+}$ in $LaCl_3$ [5] that is more than a factor of 5 shorter than the calculated purely radiative rate of the corresponding emitting state of aquated Es^{3+} [6]. It is improbable that nonradiative decay to lattice phonons accounts for this difference, given the energy gap law established for 4f state transitions of Ln^{3+} in $LaCl_3$ [7]. In comparison with $LaCl_3$, LaF_3 would be expected to less readily form color centers because of the higher electron affinity of fluorine versus chlorine atoms.

2. Experimental details

An ion-exchange column separation was used to remove decay daughter ^{249}Bk from ^{253}Es [4]. The sample was prepared by coprecipitation of Es^{3+} in LaF_3 (nominally 0.014 wt.% Es in LaF_3). The precipitate was dried under a stream of nitrogen gas, heated in anhydrous HF in a nickel tube, and then twice thermally fluorinated using fluorine gas to ensure trivalent Es. The resulting powder sample was loaded into a fused-silica capillary tube in a dry atmosphere gloved box. The sample tube then was evacuated, back filled with He gas, and flame sealed.

The sample cell was placed into the heat exchange gas space of a temperature-controlled, liquid helium-cooled cryostat. A dye laser pumped by a Q-switched Nd:YAG laser was the excitation source for time- and wavelength-resolved laser-induced fluorescence studies. A computer-interfaced, cooled, gated optical multichannel analyzer and a 1-m monochromator recorded shorter wavelength time-resolved emission spectra. The gated analyzer provided discrimination against short-lived luminescence at the recorded wavelengths by more than a factor of 10^6. Emission spectra at wavelengths longer than 900 nm were acquired using a cooled photomultiplier attached to the dual exit slit assembly of the monochromator. The dual exit slit enabled rapidly switching between these two

---

*Corresponding author. Fax: +1 630 2527393; e-mail: beitz@anlchm.chm.anl.gov1

0925-8388/98/$19.00
PII: S0925-8388(98)00232-1

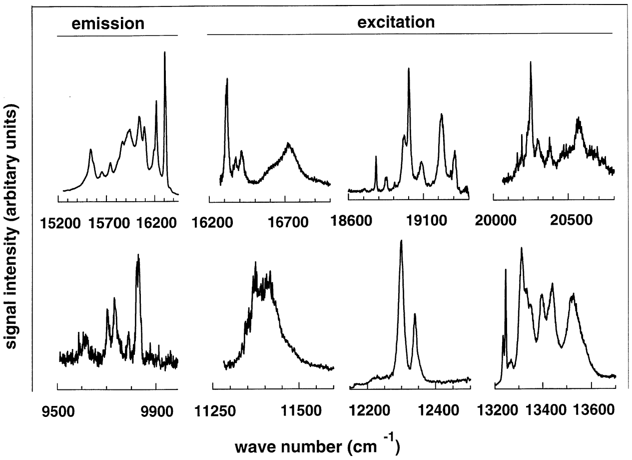

Fig. 1. Observed emission and excitation spectra of f–f transitions of Es^{3+} in LaF_3 recorded at 15 K using time- and wavelength-resolved laser-induced fluorescence techniques.

detection capabilities. Photomultiplier data were acquired using a computer-interfaced boxcar detector (for emission spectra) or a signal averaging transient recorder (for decay dynamics studies).

3. Results

Intense, short-lived luminescence (attributed to radiation-induced defects such as color centers) interfered with observation of emission from 5f states of Es^{3+} above 20 000 cm^{-1}. Some of the observed excitation and emission spectra recorded at 15 K are shown in Fig. 1. Emission spectra were recorded using 526 nm excitation. Excitation spectra for the $^5F_4$ and higher lying states were recorded by monitoring emission from the $^5F_4$ state. For other excitation spectra, $^5F_5$ state emission was monitored.

Classification of observed lines as to purely electronic or vibronic character was based on the temperature dependence of the observed spectra. The components of the $^5I_8$ ground state were assigned based on emission to it from the $^5F_4$ state and confirmed, for the lowest lying components, by emission from the $^5F_5$ state. The origin of the $^5F_4$ state was confirmed by observing it in both excitation and emission. As noted by Carnall [3], the metal ion site symmetry in LaF_3 is C_2 and, in consequence, few optical selection rules exist. Use of a powdered sample in our work prevented polarization analysis. For these reasons, state assignment was carried out starting from the premise that the free ion states deduced from work on Es^{3+} in $LaCl_3$ [1] are approximately those of Es^{3+} in LaF_3.

Nonlinear least-squares modeling of the observed spectra as to the underlying energy level structure of 5f electron states was carried out by approximating the site symmetry as C_{2v} and using an effective operator Hamiltonian formalism with simultaneous adjustment of free-ion parameters, as has been described previously [1]. The starting point for modeling was the set of crystal field parameters established for the 4f counterpart of Es^{3+}, namely Ho^{3+}, in LaF_3 [3] and the known trends for crystal field parameters of 3+ actinide ions in $LaCl_3$. Assignments of levels within a crystal field multiplet were guided by past work on Es^{3+} in $LaCl_3$ [1] and the results of preliminary model calculations. Table 1 lists the resulting best fit model parameters; Table 2 compares the resulting calculated state energies to the assigned observed bands. As is evident, the model calculation provides a good fit to the assigned levels. However, for the reasons noted above, the assignments within a multiplet and the value of the deduced crystal field parameters must be considered to be subject to future revision when crystal field parameter trends for trivalent actinides in LaF_3 become established.

The fluorescence decay of the $^5F_5$ and $^5F_4$ states of Es^{3+} in LaF_3 at 15 K were recorded and found to consist of a complex but rapid initial decay followed by a single exponential decay at longer times. The rapid initial decay of the Es^{3+} emission is attributed to the influence of radiation damage-induced color centers that quench the Es^{3+} excitation energy. The exponential decay at longer times reflects the dynamics of Es^{3+} ions that are isolated from the influence of color centers. The observed lifetimes are compared, in Table 3, with values for Es^{3+} in $LaCl_3$ [5,8] and the calculated purely radiative lifetime of the $^5F_5$

Table 1
Energy level model parameters for Es^{3+} in LaF_3 (in cm^{-1})[a]

Par.	Value	Par.	Value	Par.	Value	Par.	Value
F^2	64 570(53)	γ	472(32)	T^8	[408]	B^2_2	[−100]
F^4	50 351(140)	T^2	[110]	M^0 [b]	[1.458]	B^4_2	423(53)
F^6	38 047(89)	T^3	[45]	P^2 [c]	[506]	B^4_4	838(47)
ξ	3955(2)	T^4	[50]	B^0_2	−505(37)	B^6_2	−1163(54)
α	[30.21]	T^6	[−256]	B^4_0	1167(86)	B^6_4	−651(52)
β	−751(20)	T^7	[684]	B^6_0	351(70)	B^6_6	−1930(42)

[a] Values in parentheses are errors in indicated parameters. Value in brackets were not allowed to vary in parameter fitting.
[b] M^2 and M^4 were constrained to the ratios $M^2=0.55\ M^0$ and $M^4=0.36\ M^0$.
[c] P^4 and P^6 were constrained to the ratios $P^4=0.5\ P^2$ and $P^6=0.1\ P^2$.

Table 2
Experimental and calculated 5f state energy levels of Es^{3+} in LaF_3

Largest $^{2S+1}L_J$ state	Exp. energy[a] (cm^{-1})	Calc. energy[b] (cm^{-1})	Exp. −Calc.[c] (cm^{-1})
$^5I_8$	0	4.3	−4.3
	9.5	6.9	2.6
	41.0	41.3	−0.3
		53.2	
	125.0	126.8	−1.8
	220.0	222.3	−2.3
	282.0	262.3	19.7
		341.4	
	380.0	372.4	7.6
	461.0	479.0	−18.0
	506.0	521.2	−15.2
		538.5	
	580.0	603.5	−23.5
		630.6	
	752.0	729.3	22.7
	780.0	771.0	9.0
	783.0	779.9	3.1
$^5F_5$	9828.0	9827.9	0.1
		9844.9	
		9863.9	
		9863.9	
		9878.4	
		9922.2	
		9972.1	
		9980.1	
		9992.0	
		10 073.9	
		10 107.5	
$^5I_7$		11 053.2	
		11 070.1	
		11 089.5	
		11 127.7	
		11 134.7	
		11 172.7	
		11 190.8	
		11 191.9	
		11 195.6	
		11 229.6	
		11 261.9	
		11 282.2	
		11 300.0	
		11 308.2	
		11 351.2	
$^3D_2$	12 228.0	12 249.0	−21.0
		12 261.2	
	12 290.0	12 289.1	0.9
	12 299.0	12 291.1	7.9
	12 340.0	12 325.6	14.4
$^5I_6$	13 233.0	13 215.8	17.2
	13 244.0	13 218.3	25.7
	13 258.0	13 262.5	−4.5
	13 295.0	13 298.3	−3.3
	13 312.0	13 328.3	−16.3
	13 326.0	13 332.3	−6.3
	13 350.0	13 351.8	−1.8
	13 358.0	13 371.4	−13.4
	13 390.0	13 391.4	−1.4
	13 395.0	13 392.1	2.9
	13 440.0	13 436.5	3.5
	13 520.0	13 524.7	−4.7
	13 535.0	13 533.4	1.6
$^5F_4$	16 314.0	16 300.8	13.3
	16 321.0	16 321.7	−0.7
	16 373.0	16 385.0	−12.0
	16 416.0	16 431.8	−15.8
		16 447.2	
	16 580.0	16 574.9	5.1
	16 598.0	16 583.9	14.1
	16 629.0	16 632.7	−3.7
		16 664.5	
$^5I_4$		17 921.9	
		17 924.5	
		17 989.6	
		18 049.4	
		18 057.6	
		18 131.4	
		18 133.3	
		18 194.0	
		18 283.9	
$^5I_5$	18 707.0	18 715.5	−8.5
	18 783.0	18 799.1	−16.1
	18 855.0	18 837.6	17.4
	18 908.0	18 888.8	19.2
		18 943.5	
	18 972.0	18 973.0	−1.0
	19 006.0	19 001.1	4.9
	19 088.0	19 093.5	−5.5
	19 165.0	19 163.3	1.7
		19 291.9	
	19 309.0	19 322.5	−13.5
$^3K_8$,$^5G_6$		19 938.1	
		19 956.7	
		19 987.4	
		20 008.8	
		20 016.2	
		20 049.0	
		20 067.8	
		20 076.2	
		20 081.3	
		20 085.8	
		20 096.5	
		20 105.7	
		20 110.3	
		20 148.0	
	20 162.0	20 159.7	2.3
	20 193.0	20 212.2	−19.2
	20 228.0	20 218.9	9.1
	20 238.0	20 234.9	3.1
	20 256.0	20 248.2	7.8
	20 300.0	20 298.2	1.8
	20 320.0	20 326.2	−6.2
		20 353.3	
	20 365.0	20 364.9	0.1
	20 380.0	20 378.3	1.7
		20 405.2	
		20 454.1	
		20 501.9	
		20 506.6	
		20 516.9	
		20 521.0	

[a] Estimated uncertainty: ±2 cm^{-1}.

[b] Energies are shown for all calculated levels up to and including $^3K_8$,$^5G_6$.

[c] Considering all 56 assigned lines, the deviation [1] between the experimental and calculated values is 13.1 cm^{-1}.

Table 3
Comparison of 5f state dynamics of Es^{3+}

Es^{3+} emitting state	Energy gap (cm^{-1})[a]	Observed lifetime (μs)		Aquated Es^{3+} calculated purely radiative lifetime[d] (μs)
		Es^{3+} in $LaCl_3$[b]	Es^{3+} in LaF_3[c]	
$^5F_5$	9425	418	2060±100	2400
$^5F_4$	2970	23	39±6	Not reported

[a] Based on the free-ion state energies of Es^{3+} in $LaCl_3$ [1].
[b] At 4 K [5,8].
[c] Present work at 15 K, The long time portion of an observed decay was fit to a single exponential decay model.
[d] See Ref. [6].

state of aquated Es^{3+} [6]. It is evident in Table 3 that the observed lifetimes in LaF_3 are longer than those reported for $LaCl_3$ which is counter to the trend expected if nonradiative decay to lattice phonons (energy gap law behavior [7]) dominated the dynamics. This provides evidence that nonradiative decay to color centers or other radiation damage-induced factors dominated the 5f state dynamics of Es^{3+} in $LaCl_3$. As might be expected from energy gap law trends for trivalent lanthanide ions in LaF_3 [3], the observed lifetime of the $^5F_5$ state of Es^{3+} in LaF_3 is comparable to the calculated purely radiative lifetime of the state. Evidence that this state can undergo rapid nonradiative decay in the absence of significant radiation damage is found in the reported short observed fluorescence lifetimes of the $^5F_5$ state of Es^{3+} as an aquated ion (1.05 μs in H_2O) and complexed in a organic phase (2.34 μs) [9]. In these solution phase studies, the coordinated ligands contained high-frequency fundamental vibrational modes that are absent in LaF_3.

Acknowledgements

The Transplutonium Element Program at Oak Ridge National Laboratory supplied the ^{253}Es used in this work. J.V.B. thanks L.R. Morss for providing a temperature-controlled ion-exchange column system and instruction in its use. This work was performed under the auspices of the Office of Basic Energy Sciences, Division of Chemical Sciences of the US Department of Energy under contract W-31-109-ENG-38.

References

[1] W.T. Carnall, J. Chem. Phys. 96 (1992) 8713.
[2] G.H. Dieke, Spectra and Energy Levels of Rare Earth Ions in Crystals, Interscience, New York, 1968.
[3] W.T. Carnall, G.L. Goodman, K. Rajnak, R.S. Rana, J. Chem. Phys. 90 (1989) 3443.
[4] E.K. Hulet, in: J.J. Katz, G.T. Seaborg, L.R. Morss (Eds.), The Chemistry of the Actinide Elements, 2nd ed., vol. 2, Chapman and Hall, London, 1986, pp. 1071–1084.
[5] J.P. Hessler, private communication.
[6] W.T. Carnall, H.M. Crosswhite, in: J.J. Katz, G.T. Seaborg, L.R. Morss (Eds.), The Chemistry of the Actinide Elements, 2nd ed., vol. 2, Chapman and Hall, London, 1986, pp. 1235–1277.
[7] H.W. Moos, J. Lumin. 1 (1970) 106.
[8] J.P. Hessler, J.A. Caird, W.T. Carnall, H.M. Crosswhite, R.K. Sjoblom, F. Wagner Jr., in: G.J. McCarthy, J.J. Rhyne (Eds.), The Rare Earths in Modern Science and Technology, Plenum, New York, 1978, pp. 507–512.
[9] J.V. Beitz, D.W. Wester, C.W. Williams, J. Less-Common Metals 93 (1983) 331.